

Neuronal Quantification of Subthalamic Nucleus in Adult Human Cadaveric Brain- A Histological Study

MANGALA KOHLI¹, REEHA MAHAJAN², PA ATHIRA³



ABSTRACT

Introduction: The Subthalamic Nucleus (STN) has emerged as a preferred target site for deep brain stimulation for various neurological disorders. There is scarcity of literature on the internal structure of subthalamic nucleus.

Aim: To study its microanatomy and quantification of its various cells in different age groups.

Materials and Methods: The study design of the current study is of cross-sectional type which was done on 30 cadaveric brains in Anatomy department of Lady Hardinge medical college, New Delhi which were divided into three age groups ranging from 20 to >50 years. The subthalamic nucleus was fixed and subjected to standard tissue processing procedure. The sections were stained with Haematoxylin and Eosin (H&E), Nissl and Haggqvist staining. The neurons and neuroglia were studied in 25 representative areas, measuring

75166 μm^2 in each age group, using the upright binocular optical microscope and image analysis software. The number of neurons and neuroglia with their ratio was calculated and results were statistically analysed using Microsoft Excel software (2010 version).

Results: Three types of neurons were identified as multipolar, fusiform and pear-shaped neurons. The ratio of neuroglia to neurons in the three age groups was calculated as: Group A-9.197, Group B-9.274 and Group C-10.478. A p-value of 0.04 was observed on comparing the neuronal and neuroglial density in Group A and C, demonstrating a significant increase in the density of neuroglia with age.

Conclusion: The results obtained in the present study can provide prerequisite knowledge to anatomists, pathologists, and neurosurgeons for detection of various pathologies and interventional procedures, respectively.

Keywords: Histology, Neuroglia, Neuron

INTRODUCTION

The subthalamic nucleus is group of neurons within the cerebrum and is a key component of the basal ganglia. It is placed inferior to the thalamus. In humans, the nucleus is estimated to contain approximately 5,50,000 projection neurons which include large multipolar neurons, fusiform cells and small interneurons [1]. Subthalamic nucleus has been associated with various neurological disorders, such as, Parkinson's disease and obsessive compulsive disorder [2]. The STN has also emerged recently as a preferred target site for deep brain stimulation in obsessive compulsive disorder [3]. The histology of STN in humans has not been extensively studied by the researchers. Due to scarcity of literature on the internal structure of STN, the present study aims to study the morphology of different types of neurons present in STN and the quantification of neurons and neuroglia in different age groups. The morphometry of STN in the right and left hemispheres of the same age groups has already been reported in our previous study [4]. This study will give an insight to the neurosurgeons about the ratio of neurons and neuroglia in STN, for targeting during various invasive and non-invasive procedures in different age groups.

MATERIALS AND METHODS

The study design of the current study is of cross-sectional type which was done on 30 cadaveric brains in Anatomy department of Lady Hardinge medical college, New Delhi from 2014-15 over a span of 18 months. The brain specimens were obtained from unclaimed and donated bodies procured from Forensic medicine department of Lady Hardinge Medical College, New Delhi. These brain specimens were retrieved from the donated and unclaimed bodies with known cause of death. The brain

specimens with suspected STN involvement were rejected. The specimens were divided into three age groups with 10 specimens in each group: Group A: 20-35 years, Group B: 35-50 years and Group C: above 50 years. All samples were collected after following the standard protocol for ethical clearance obtained from Institutional Ethics Committee (Ref. no.LHMC/ECHR/2014/446, dated 31.10.2014).

Inclusion criteria: The cadaveric brains with known cause of death and appearing normal on gross examination were included in the study.

Exclusion criteria: The cadaveric brains obtained from individuals with history of neurological disorders were rejected.

The cadaveric brains were removed en masse from the body and immediately fixed in 10% formalin. The STN along with the surrounding tissue was taken from the brain specimens and fixed in 10% formalin for seven days. The grossing of the tissue was done by cutting the specimen into sections with thickness of 5 mm for preparation of paraffin blocks. The tissues were then processed for paraffin embedding, following the protocol described below.

Protocol for Processing, Embedding and Section Cutting

All the cut sections were washed thoroughly with tap water and subjected to dehydration with ascending grades of alcohol (70% alcohol for 90 minutes, 80% alcohol for 90 minutes, 90% alcohol for 90 minutes, Absolute alcohol I for one hour, Absolute alcohol II for one hour and 100% Acetone for five minutes). Then, it was immersed in cedar wood oil for clearing (overnight) and dipped in chloroform for 20 min and chloroform: paraffin wax (50:50) at 64°C for 30 minutes. Then, it was embedded in paraffin wax at 64°C (Paraffin wax I- one hour and Paraffin wax

11-one hour). The paraffin blocks were prepared using plastic moulds. The block was then trimmed for sectioning. The tissue was sectioned at 6 µm thickness using a rotary microtome. The sections were floated on a warm water bath for spreading out and lifted on glass slides pre-smearred with egg albumin and thymol. All the steps in tissue processing were handled with extreme care to minimise damage to the tissues. The following staining procedures were done:

1. Haematoxylin & Eosin staining (H&E staining)
2. Nissl staining
3. Haggqvist staining

1. Haematoxylin and Eosin Stain

a. Harris' haematoxylin: It is a powerful and selective nuclear stain which gives sharp delineation of nuclear structure.

b. Eosin: A red dye, when properly used on well-fixed material, stains connective tissue and cytoplasm in varying intensity and shades of the primary colour, giving a most useful differential stain. A 1% eosin was used as the working solution.

Staining technique: Slides were deparaffinised and hydrated by passing through descending grades of ethanol. Staining was carried out in aqueous solution of haematoxylin for 10-15 minutes. The slides were washed in tap water for 5-7 minutes followed by dip in 1% acid alcohol. The slides were again washed in running water (5-10 minutes) for bluing. For eosin staining, the slides were dipped in 0.5% alcoholic solution of eosin (10-15 seconds). Final dehydration was done in ascending grades of alcohol and two changes in acetone (2 minutes each). Clearing was done by immersing the slides in xylene. The slides were then cover slipped using Dibutylphthalate Polystyrene Xylene (DPX) as the mountant.

2. Nissl Staining or Cresyl Violet Stain

Cresyl violet is a basic dye that binds to nucleic acids, like DNA and RNA. It is used in neural tissue to demonstrate rough endoplasmic reticulum, also called the Nissl substance. Cresyl violet staining helps in the measurement of density of neurons.

It was prepared using cresyl violet acetate (0.1 g), distilled water 100 mL, and 10 drops of glacial acetic acid were added just before use and filtered to form 0.1% cresyl violet solution.

3. Haggqvist Staining

This is a special staining technique used for nervous tissue [5]. This delineates the cell shape and structure clearly along with its axon.

a. Baker's fixative: It is used as a postfixative. It is prepared using 100 mL formalin, 900 mL tap water and 20 g Calcium chloride.

b. Mann's solution: It is a mixture of two anion dyes, eosin and methyl blue. It is prepared using methyl blue 0.2%, Eosin Y 0.25%, distilled water and absolute alcohol. The brain specimen is initially fixed in 10% formalin for four weeks. The subthalamic tissue was dissected out and was post-fixed in bakers fixative for six weeks. Tissue was mordanted in six-eight changes of potassium dichromate. The tissue was then embedded in paraffin wax and sections of 6 µm thickness were cut. Sections were deparaffinised and placed in 10% phosphomolybdic acid for 30 minutes. The slides were stained in Mann's solution for ten minutes and differentiated in 70% ethanol for two minutes followed by dehydration in 96% and 100% ethanol for two minutes each and clearing in two changes of xylene for five minutes each. The slide was mounted in DPX.

These three staining procedures were performed to study the microscopic structure of STN highlighting the morphology of neurons. The shape and structure of neurons were studied using the three techniques of staining because Nissl staining and

Haggqvist staining are helpful in highlighting the Nissl substance and delineating the cell shapes clearly and can support the findings of H&E staining. The neurons and neuroglia were studied in the H&E stained sections of the STN in 25 representative areas in all the three age groups. The area of the counting frame was fixed as 75166 µm². Each representative area measured 75166 µm² and all areas were studied using the upright binocular optical microscope (Olympus DSX 1000) with digital camera and image analysis software. The neuron and neuroglia densities were calculated by counting their numbers in 25 representative areas for each age group at 20X magnification.

STATISTICAL ANALYSIS

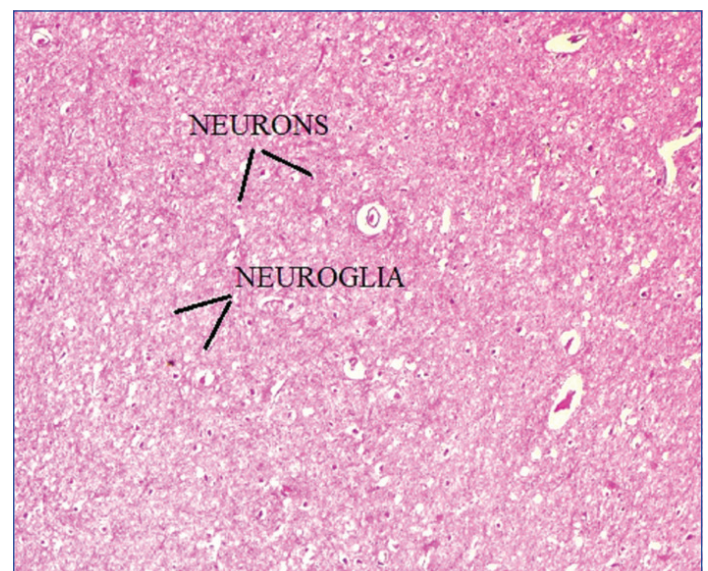
The number of neurons and neuroglia and their ratio was calculated using image analyser software (Image J version 1.43) and the results were statistically analysed and tabulated using Microsoft Excel version 2010. A p-value <0.05 was considered as significant.

RESULTS

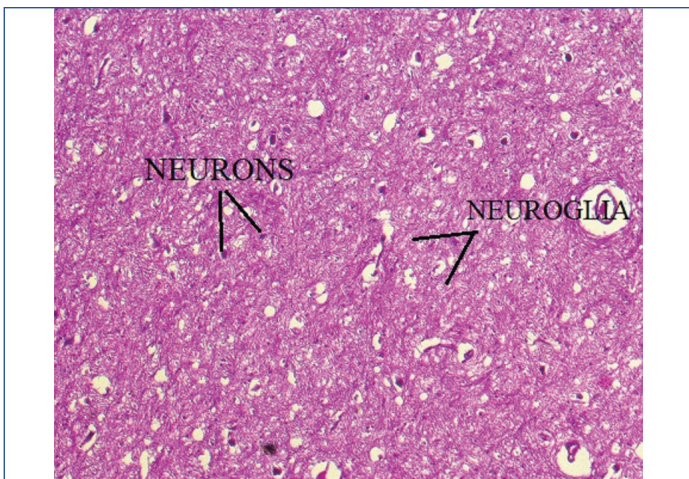
Under low power(10X) objective, in all the stained sections, neurons and neuroglia cells could be easily differentiated and were seen scattered throughout the nucleus [Table/Fig-1,2]. The neuronal cell body had spaces around it and this is a common artefact seen in formalin-fixed tissue that is dehydrated and embedded in paraffin wax. This occurs due to the differential shrinkage of the neuronal soma. The neurons were surrounded by bundles of axons and numerous neuroglia. The neuroglia was smaller in size and identified as small oval structures embedded in the nerve fibres. Three types of neurons could be identified in the STN and based on the morphology they were classified into:

- a) Multipolar neurons: The soma of the neurons was triangular or quadrangular in shape. Neuronal processes could be seen radiating from the cell body. This type of cell was found in all parts of the nucleus and was the most abundant [Table/Fig-3].
- b) Neurons with fusiform cell body were found mainly in the periphery of the nucleus. The neuronal processes were observed to arise from opposite poles [Table/Fig-4].
- c) Pear-shaped neurons were visualised in the central region of the STN. Neuronal processes were observed to arise from one pole of the soma [Table/Fig-5].

The Nissl- stained sections showed a similar morphology as the H&E stain. Abundant Nissl granules which are rough endoplasmic reticulum were observed in the cytoplasm of the neurons. The



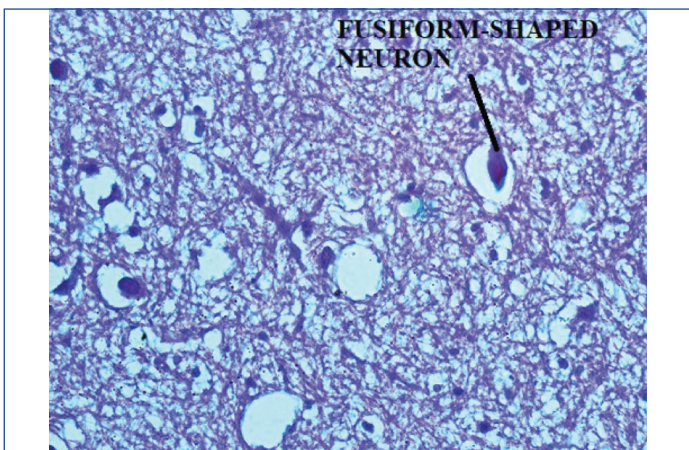
[Table/Fig-1]: Haematoxylin and Eosin staining showing neurons, neuroglia and nerve fibres (100X).



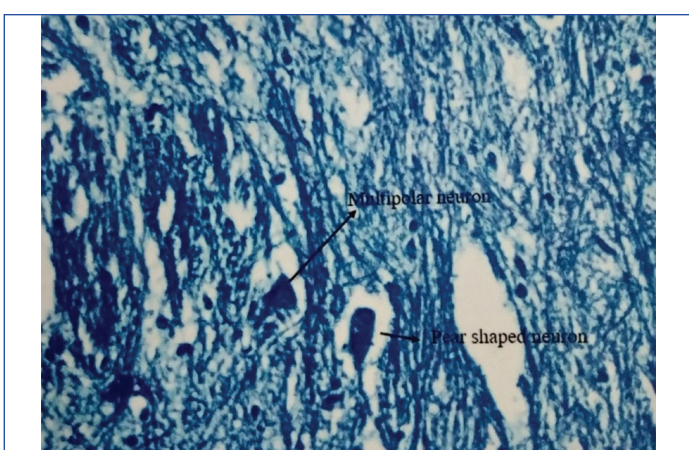
[Table/Fig-2]: Haematoxylin and Eosin staining showing neurons, neuroglia and nerve fibres (400X).



[Table/Fig-3]: Haematoxylin and Eosin staining showing multipolar neurons (400X).

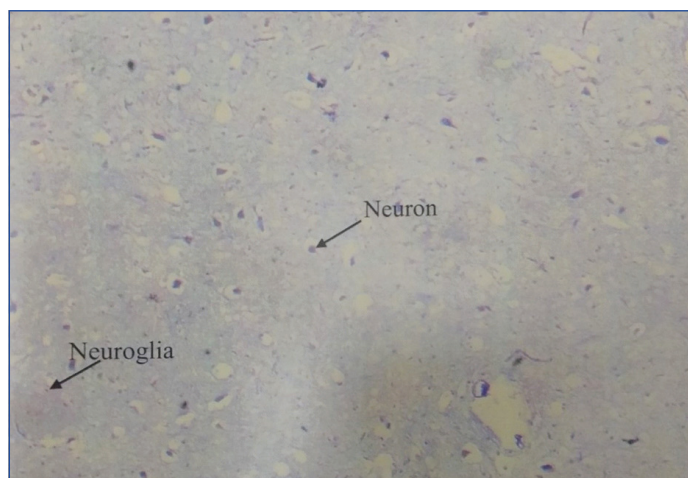


[Table/Fig-4]: Haggqvist staining showing fusiform neurons (400X).

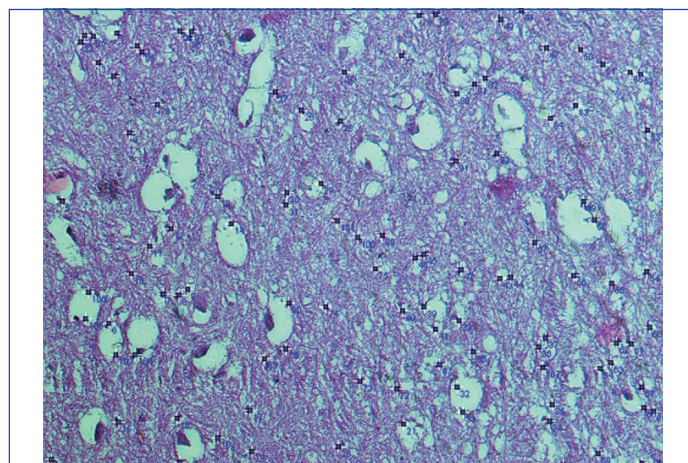


[Table/Fig-5]: Haggqvist staining showing pear-shaped and multipolar neurons (400X).

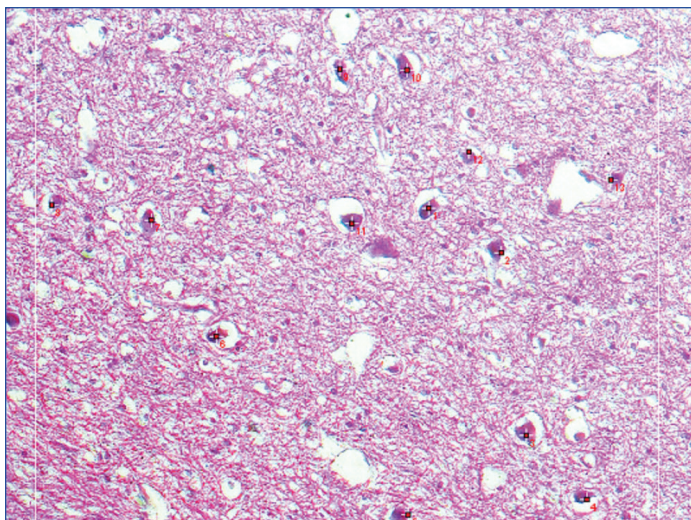
neurons had a large centrally placed nucleus. The three types of neurons observed in the H&E stain could be visualised in Nissl staining also [Table/Fig-6]. In the Haggqvist-stained sections, the neurons appeared blue in colour. The mean number of neurons and neuroglia were also counted in 75166 μm^2 field using Image J software [Table/Fig-7,8]. The count of neurons and neuroglia in 25 representative fields (75166 μm^2 area each) for Group A, B and C is shown in [Table/Fig-9] which is a line charts with markers, in which the X-axis shows the 25 representative field areas and the Y-axis depicts the number of neurons and neuroglia counted in each field for each group. In Group A, the mean number of neurons per 75166 μm^2 was calculated to be 10.28 i.e., 136.76 neurons/mm². The mean number of neuroglia per 75166 μm^2 was calculated to be 94.52 i.e., 1257.83 neuroglia/mm² [Table/Fig-10]. The ratio of neurons to neuroglia in Group A was observed to be 9.1971. In group B, the mean number of neurons per 75166 μm^2 was calculated to be 10.2 i.e., 135.69 neurons/mm². The mean number of neuroglia per 75166 μm^2 was calculated to be 94.6 i.e., 1258.55 neuroglia/mm² [Table/Fig-10]. The ratio of neurons to neuroglia in Group B was observed to be 9.2745. In Group C, the mean number of neurons per 75166 μm^2 was calculated to be 10.04 i.e., 133.57 neurons/mm². The mean number of neuroglia per 75166 μm^2 was calculated to be 105.2 i.e., 1399.57 neuroglia/mm² [Table/Fig-11]. The ratio of neurons to neuroglia in Group C was observed to be 10.478. The p-value suggests that there is no significant change in the density of neurons and neuroglia between Group A and Group B [Table/Fig-10]. A significant p-value (0.04) was observed on comparing the neuronal and neuroglial density in Group A and C which shows a significant increase in the density of neuroglia with age [Table/Fig-11]. As per the p-value, there is no significant change in the density of neurons and neuroglia between Group B and Group C [Table/Fig-12].



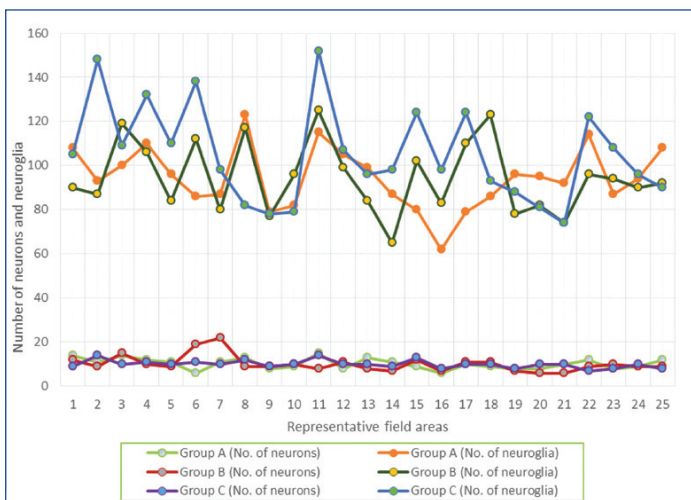
[Table/Fig-6]: Nissl staining showing neurons, neuroglia and nerve fibres (100X).



[Table/Fig-7]: Demonstration of neuron counting in 75166 μm^2 area using Image J software (400X).



[Table/Fig-8]: Demonstration of neuroglia counting in 75166 μm² area using Image J software (400X).



[Table/Fig-9]: Line diagram with markers showing number of neurons and neuroglia in 25 representative fields in Group A, B and C.

Parameter	Group A			Group B			p-value
	Mean	SD	SE	Mean	SD	SE	
No. of Neurons	10.28	2.46	0.492	10.2	3.73	0.75	0.9290
No. of Neuroglia	94.52	13.86	2.771	94.6	16.202	3.24	0.9851

[Table/Fig-10]: Comparison of neuronal and neuroglial density in Group A and Group B using unpaired t-test. SD: Standard deviation; SE: Standard error

Parameter	Group A			Group C			p-value
	Mean	SD	SE	Mean	SD	SE	
No. of Neurons	10.28	2.46	0.492	10.04	1.77	0.353	0.6936
No. of Neuroglia	94.52	13.86	2.771	105.2	21.77	4.35	0.0439

[Table/Fig-11]: Comparison of neuronal and neuroglial density in Group A and Group C using unpaired t-test. SD: Standard deviation; SE: Standard error

Parameter	Group B			Group C			p-value
	Mean	SD	SE	Mean	SD	SE	
No. of Neurons	10.2	3.73	0.746	10.04	1.77	0.353	0.8471
No. of Neuroglia	94.6	16.2	3.24	105.2	21.77	4.35	0.0567

[Table/Fig-12]: Comparison of neuronal and neuroglial density in Group B and Group C using unpaired t-test. SD: Standard deviation; SE: Standard error

DISCUSSION

The histology of the STN in humans has not been studied extensively, though studies involving mammals and lower animals have been conducted. In the current study, the morphology of the neurons

was studied with the help of haematoxylin and eosin stain, Nissl's stain and Haggqvist staining method. Three types of neurons have been recognised in the present study based on the morphology- multipolar neurons with triangular soma, fusiform neurons and pear-shaped neurons. These morphological characteristics were similar to the neurons reported by Robak A et al., in Guinea pigs [6]. Robak A et al., reported three types of neurons: Type I or multipolar neurons with four-six dendrites and triangular or quadrangular soma, Type II or bipolar neurons with fusiform perikarya with dendrites arising from opposite poles and type III or pear-shaped neurons with thick dendritic trunks arising from one pole. Since special staining for axons and dendrites were not done in the present study, the branching pattern reported by Robak A et al., could not be compared. However, the fusiform neurons were mainly present in the peripheral region of STN in the current study which is comparable with the findings of Robak A et al. [6]. Comparable results were also reported by Afsharpour S, who conducted the microanatomic study on rat STN using Golgi technique and Nissl stain [7]. Some researchers conducted electron microscopic study of the primate STN and reported two types of principal neurons in the STN: radiating and fusiform [8,9]. However, scanning of literature reveals no evidence of such studies on human cadaveric brains.

As per the study conducted by Chang HT et al., neurons of STN are abundant in mitochondria, lysosomes, ribosomes and golgi apparatus but have sparse endoplasmic reticulum [10]. These findings of internal structure of STN cannot be compared with the present study, as it was conducted under electron microscopy.

The present study calculated the number of neurons and neuroglia per mm² of the nucleus. It was observed that though there was a reduction in the number of neurons per mm² with increasing age; this was not statistically significant. This is in accordance with the study conducted by Sturrock RR, who studied the stability of neuron number in the STN and reported that there was no significant variation in the number of neurons or its morphology with advancing age [11]. Similar study has been conducted by Lange H et al., who has done a morphometric analysis of the STN on 14 cerebral hemispheres in which density of neurons was observed to be 1970±145 neurons/mm³ in the lateral part of the nucleus and 2910±310 neurons/mm³ in the medial part. The mean volume of the cells in the lateral portion was 8070 mm³ and 6960 mm³ in medial part, while the comparison of densities of various cells in medial and lateral portion of STN has not been done in the present study [12].

In the current study, the ratio of the neurons to neuroglia has been compared in three different age groups. The present study observed that there is a significant increase in the glial cell number with advancing age. This could be because gliosis is a sign of ageing. The age group variation, in the STN internal structural architecture has not been reported in the available literature.

Various immunological studies depicting the presence of various receptors responsible for the functioning of STN have been conducted [5,13-16]. One of the researcher has tried to determine the intricate anatomical structure of STN with the help of fiber dissection and 3D magnetic resonance imaging reconstruction, but thorough examining of literature has revealed a dearth of studies on the histological structure and neuronal quantification of STN [17].

Limitation(s)

The number of cadaveric brains taken in each group is small and the comparison between number of neurons and neuroglia in the right and left subthalamic nuclei has not been done in the present study. Furthermore, stereological analysis could have been done to measure the volume of STN and neuron densities in each group for correlation of findings with the existing literature and to record variations between Indian and western population.

CONCLUSION(S)

The results of the present study can provide crucial pre-requisite knowledge to the anatomists, as well as pathologists studying various sections of STN and its pathologies. The neuronal quantification observed in different age groups will give an insight to the neurosurgeons before targeting the neurons of STN during deep brain stimulation and other neurological procedures.

REFERENCES

- [1] Massey LA, Yousry TA. Anatomy of the substantia nigra and subthalamic nucleus on MR imaging. *Neuroimaging Clin N Am*. 2010;20(1):07-27.
- [2] Alexander GE. Biology of Parkinson's disease: Pathogenesis and pathophysiology of a multisystem neurodegenerative disorder. *Dialogues Clin Neurosci*. 2004;6(3):259-80.
- [3] Chabardès S, Polosan M, Krack P, Bastin J, Krainik A, David O, et al. Deep brain stimulation for obsessive-compulsive disorder: Subthalamic nucleus target. *World Neurosurg*. 2013;80(3-4):01-08.
- [4] Kohli M, Athira PA, Mahajan R. Morphometric study of subthalamic nucleus in adult human cadaveric brain. *Int J Health Sci Res*. 2018;8(6):47-51.
- [5] Swanger S, Vance K, Pare J, Sotty F, Fog K, Smith Y, et al. NMDA Receptors Containing the GluN2D subunit control neuronal function in the subthalamic nucleus. *J Neurosci*. 2015;35(48):15971-83.
- [6] Robak A, Bogus-Nowakowska K, Sztayn S. Types of neurons of the subthalamic nucleus and zona incerta in the guinea pig-Nissl and Golgi study. *Folia Morphol (Warsz)*. 2000;59(4):271-77.
- [7] Afsharpour S. Topographical projections of the cerebral cortex to the subthalamic nucleus. *J Comp Neurol*. 1985;236(1):14-28.
- [8] Rafols JE, Fox CA. The neurons in the primate subthalamic nucleus: A Golgi and electron microscopic study. *J Comp Neurol*. 1976;168:75-112.
- [9] Larsen M, Bjarkam C, Ostergaard K, West MJ, Sørensen JC. The anatomy of the porcine subthalamic nucleus evaluated with immunohistochemistry and design-based stereology. *Anat Embryol (Berl)*. 2004;208(3):239-47.
- [10] Chang HT, Kita H, Kitai ST. The ultrastructural morphology of the subthalamic-nigral axon terminals intracellularly labeled with horseradish peroxidase. *Brain Res*. 1984;299:182-85.
- [11] Sturrock RR. Stability of neuron number in the subthalamic and entopeduncular nuclei of the ageing mouse brain. *J Anat*. 1991;179:67-73.
- [12] Lange H, Thormer G, Hopf A. Morphometric-statistical structure analysis of human striatum, pallidum and nucleus subthalamicus. III. Nucleus subthalamicus. *J Hirnforsch*. 1976;17(1):31-41.
- [13] Santos-Lobato B, Del-Bel E, Pittella J, Tumas V. Cytoarchitecture of nitrenergic neurons in the human striatum and subthalamic nucleus. *Brain Res Bull*. 2016;124:129-35.
- [14] Lévesque J, Parent A. GABAergic interneurons in human subthalamic nucleus. *Mov Disord*. 2005;20(5):574-84.
- [15] Wang XS, Ong WY, Lee HK, Haganir RL. A light and electron microscopic study of glutamate receptors in the monkey subthalamic nucleus. *J Neurocytol*. 2000;29:743-54.
- [16] Alkemade A, de Hollander G, Miletic S, Keuken MC, Balesar R, de Boer O, et al. The functional microscopic neuroanatomy of the human subthalamic nucleus. *Brain Struct Funct*. 2019;224:3213-27. <https://doi.org/10.1007/s00429-019-01960-3>.
- [17] Güngör A, Baydin ŞS, Holanda VM, Middlebrooks EH, Isler C, Tugcu B, et al. Microsurgical anatomy of the subthalamic nucleus: Correlating fiber dissection results with 3-T magnetic resonance imaging using neuronavigation. *J Neurosurg*. 2018;130(3):716-32. doi:10.3171/2017.10. JNS171513.

PARTICULARS OF CONTRIBUTORS:

1. Director Professor and Ex-Head, Department of Anatomy, VMCC and Safdarjung Hospital, New Delhi, India.
2. Assistant Professor, Department of Anatomy, Al-Falah School of Medical Science and Research Centre, Faridabad, Haryana, India.
3. Junior Resident, Department of General Medicine, SKS Hospital, Salem, Tamil Nadu, India.

NAME, ADDRESS, E-MAIL ID OF THE CORRESPONDING AUTHOR:

Dr. Reeha Mahajan,
Flat No. 13, Block No. 15, Al-Falah University Campus, Dhauj,
Faridabad-121004, Haryana, India.
E-mail: mahajan.reeha@gmail.com

PLAGIARISM CHECKING METHODS: [Jain H et al.]

- Plagiarism X-checker: Aug 08, 2020
- Manual Googling: Oct 18, 2020
- iThenticate Software: Dec 28, 2020 (7%)

ETYMOLOGY: Author Origin

AUTHOR DECLARATION:

- Financial or Other Competing Interests: None
- Was Ethics Committee Approval obtained for this study? Yes
- Was informed consent obtained from the subjects involved in the study? NA
- For any images presented appropriate consent has been obtained from the subjects. NA

Date of Submission: **Aug 02, 2020**

Date of Peer Review: **Sep 23, 2020**

Date of Acceptance: **Oct 26, 2020**

Date of Publishing: **Jan 01, 2021**